6121-7904-RU-000

BSD-TDR-64-16

THERMAL RADIATION FROM THE EXHAUST PLUME OF AN ALUMINIZED COMPOSITE PROPELLANT ROCKET

By S. J. Morizumi and H. J. Carpenter

JANUARY 1964

Contract No. AF 04(694)-1

Prepared for
HQ BALLISTIC SYSTEMS DIVISION
AIR FORCE SYSTEMS COMMAND
UNITED STATES AIR FORCE
Norton Air Force Base, California

TRW SPACE TECHNOLOGY LABORATORIES
THOMPSON RAMO WOOLDRIDGE INC.

BSD-TDR-64-16 6121-7904-RU-000

THERMAL RADIATION FROM THE EXHAUST PLUME OF AN ALUMINIZED COMPOSITE PROPELLANT ROCKET

Technical Report

Prepared For

Headquarters
Ballistic Systems Division
Air Force Systems Command
United States Air Force
Norton Air Force Base, California

Contract No. AF 04(694)-1

January 1964

Prepared by:

S. J. Morizumi

H. J. Carpenter

Approved by:

I. N. Spielberg

AEROSCIENCES LABORATORY
AERODYNAMICS DEPARTMENT

SPACE TECHNOLOGY LABORATORIES
THOMPSON RAMO WOOLDRIDGE INC
ONE SPACE PARK · REDONDO BEACH, CALIFORNIA

DDC AVAILABILITY NOTICE

Qualified requestors may obtain copies of this report from the Defense Documentation Center, Cameron Station, Alexandria, Virginia 22314.

CONTENTS

FOREWORD

The authors wish to express appreciation for the helpful discussions held with numerous members of the STL Technical Staff, and particularly for the computational assistance provided by Fern R. Bright and Mary L. Persons.

SUMMARY

A technique is developed for calculating rocket base heating and spacecraft heating environments due to particle radiation from a single nozzle rocket exhaust plume. The technique has proved successful when applied to a single nozzle exhausting into a rarefied atmosphere on the basis of comparison of predictions with experimental results.

The analysis treats radiation from a cloud of particles as that from an equivalent radiating surface. Thus, the problem is reduced to the determination of the proper values of the apparent surface emissivity and the effective temperature. The particle flow field information (particle concentrations, temperatures, and trajectories) necessary to determine these two quantities is provided by a two-phase flow field computer program developed by STL.

In defining the apparent emissivity of the particle plume, an analogy with neutron scattering for a cylindrical cloud is adopted which shows the apparent emissivity to be dependent on particle emissivity and cloud optical thickness. Since the plume is non-uniform in particle size, concentration, and temperature, certain averaging techniques are used to define mean values of optical thickness and temperature.

NOMENCLATURE

Symbols

$a = \frac{2\pi r_p}{\lambda}$

E = photon (radiant energy) flux, Btu/ft^2-sec

$\tilde{E}$ = integroexponential function (Equation 18)

F = shape factor from unshaded portion of the particle plume to a surface element

I = radiant intensity, Btu/ft^2-sec-steradian-micron

k = cosine distribution exponent (Equation 7)

L = total length of path across a particle plume, ft

L_o = distance along view path from a surface element to the particle plume boundary, ft

ℓ = length through a particle plume, ft

m = number of plume segments

N = particle concentration, particles/ft^3

$P_{i-1,k}$ = collision probability (Equation 2)

$P_n \equiv P_{n,k}$

p_c = rocket chamber pressure, psia

p_e = ambient pressure, psia

Q = efficiency factor (Equation 23)

$\dot{q}$ = radiant heat rate, Btu/ft^2-sec

r = particle radius, ft or microns

T = absolute temperature, ^oR

x = distance along path from the boundary of a particle cloud, ft

$z = x \cos \theta$ (Figure 3)

α = absorptivity

β = neutron blackness (Equation 2)

γ = angle of the plane of view with respect to the plume axis, degrees

NOMENCLATURE (Continued)

Symbols

ϵ = emissivity

η = temperature averaging factor

θ = directional angle, degrees (Figure 3)

λ = wavelength, ft or microns

μ = cos θ

$\prod$ = infinite product symbol

ρ = reflectivity

σ = cross section, ft^2

σ_b = Stefan-Boltzman constant, $Btu/ft^2\text{-}sec - {}^oR^4$

τ = optical thickness

ϕ = dummy variable in integroexponential function; represents τ as used herein

Subscripts

a = apparent

i = dummy number

m = number of plume segments

M = maximum

n = dummy number

o = initial or incident

p = particle

s = scattering

t = total or extinction

tr = transmitted

α = absorbed

λ = function of wavelength

Superscripts

— = average or effective

I. INTRODUCTION

The employment of single nozzle, aluminized composite propellant rockets to boost suborbital payloads or to inject spacecraft into final orbits results in primarily radiant heating from the rocket exhaust to the boost rocket base and to the spacecraft. It is important that the heat rates be predictable to permit efficient design of thermal insulation and shielding and to permit evaluation of the effects of such heating on spacecraft solar cells, sensors, etc.

If the altitude range is restricted to that experienced by the latter stages of boosters and above, it can be shown that heating of surfaces located forward of the rocket nozzle exit due to exhaust gas radiation is negligible compared to heating from aluminum oxide particle radiation. This is true because of the relatively low temperature and emissivity of the expanded gases. The problem, then, is reduced to that of predicting the thermal radiation from the exhausted particle stream or "plume" to the surface in question. A technique sufficiently accurate for engineering design purposes has been developed and is the subject of this paper.

The approach has been to treat the cloud of particles which forms the plume as an equivalent surface radiator whose shape is that of the plume. To account for variations in radiation intensity along the surface of the plume as seen by the surface element being heated, the plume is divided into a number of segments by planes emanating from that element (Figure 1). The increment of radiation incident to the surface element from each segment is determined by the familiar relation

$$\Delta \dot{q}_i = \Delta F_i \, \bar{\epsilon}_{a_i} \, \sigma_b \, \bar{T}_i^{\,4} \qquad (1)$$

A summation of radiation from all segments visible to the surface element yields the value of the total radiation.

The shape factor, ΔF_i, of each segment to the surface element is a function of the surface shape of the particle plume. Morizumi[1] has developed an analytical method for calculating shape factors to cones, hyperboloids, and segments thereof, which has been employed to arrive at the values used herein.

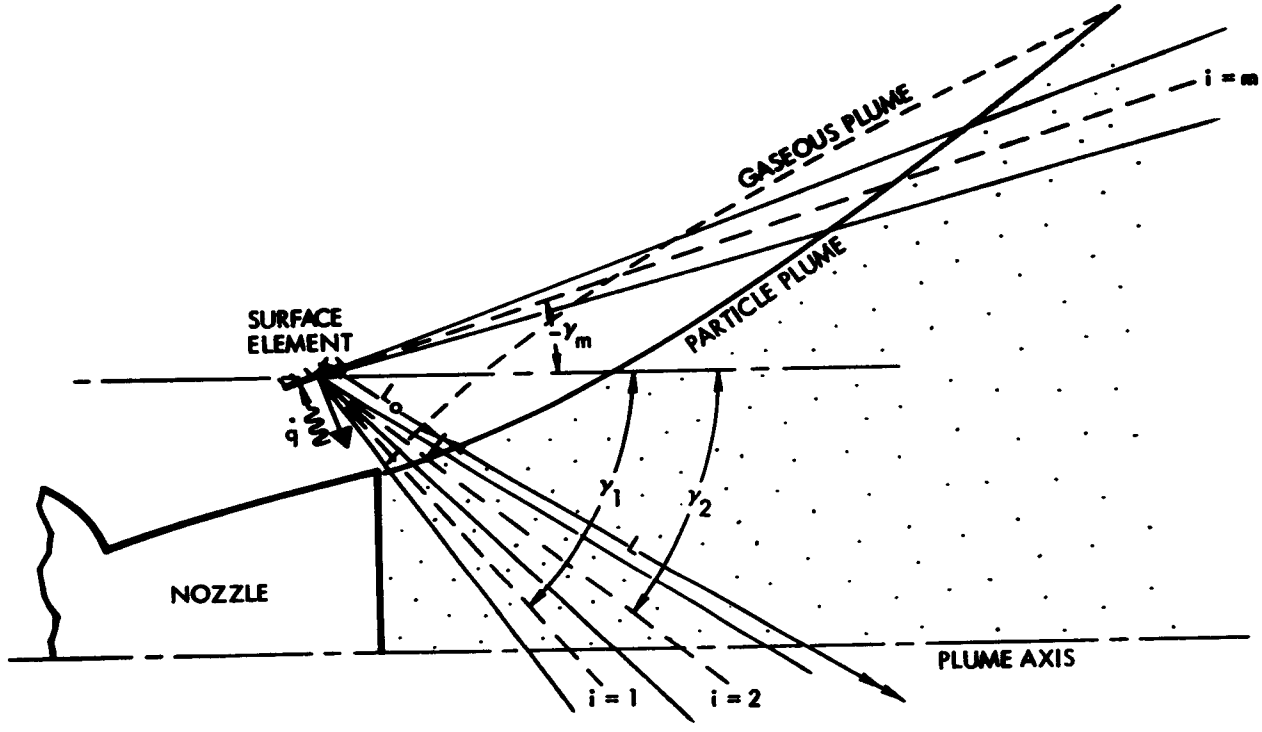

Figure 1. Sketch of Nozzle with Gaseous and Particle Plumes, and Surface Element of Base Region

The remaining two quantities to be determined in Equation (1), $\bar{\epsilon}_{a_i}$ and $\bar{T}_i^4$, are functions of not only the surface shape of the plume, but also the aluminum oxide particle concentrations and temperatures. The methods used to determine these two quantities are discussed here in detail.

Techniques used to arrive at all three quantities rely upon particle flow field information (particle trajectories, concentrations, and temperatures). The flow field is described by a two phase flow computer program developed by Kliegel and Nickerson.[2]

II. ANALYTICAL METHOD

A. APPARENT EMISSIVITY

1. Analogy with Neutron Scattering

In determining the apparent emissivity of a particle cloud, an analogy with neutron blackness (probability of neutron absorption by a medium) is used. The neutron blackness utilizing the probability approach is expressed by Stewart[3,4] and Anthony[5] in their studies of the neutron scattering problem as

$$\beta = \left(\frac{\sigma_a}{\sigma_t}\right) \sum_{j=1}^{\infty} \left(\frac{\sigma_s}{\sigma_t}\right)^{j-1} \prod_{i=1}^{j} P_{i-1,k}(\tau) \qquad (2)$$

The collision probability $P_{i-1,k}$ is defined as the probability that a neutron which has experienced (i - 1) collisions with other particles in the medium will experience at least one more collision therein. As shown in References 3, 4, and 5, the collision probability increases monotonically with optical thickness; the latter is a measure of capture probability and is defined in the following section.

A similar probability function can be used to define the radiant energy absorbed by a cloud of particles. In this case, the photons in the particle cloud are considered to replace the neutrons. As illustrated in Figure 2, the radiant energy absorbed in the first collision of photons with particles is

$$\Delta E_{a_1} = E_o \left[P_o - P_o \rho_p\right] = E_o P_o (1 - \rho_p).$$

Likewise, the energy absorbed on each successive collision is

$$\Delta E_{a_2} = E_o P_o P_1 \rho_p (1 - \rho_p)$$

$$\Delta E_{a_3} = E_o P_o P_1 P_2 \rho_p^2 (1 - \rho_p)$$

$$\vdots \qquad\qquad \vdots$$

$$\Delta E_{a_n} = E_o P_o P_1 \cdots P_{n-1} \rho_p^{n-1} (1 - \rho_p).$$

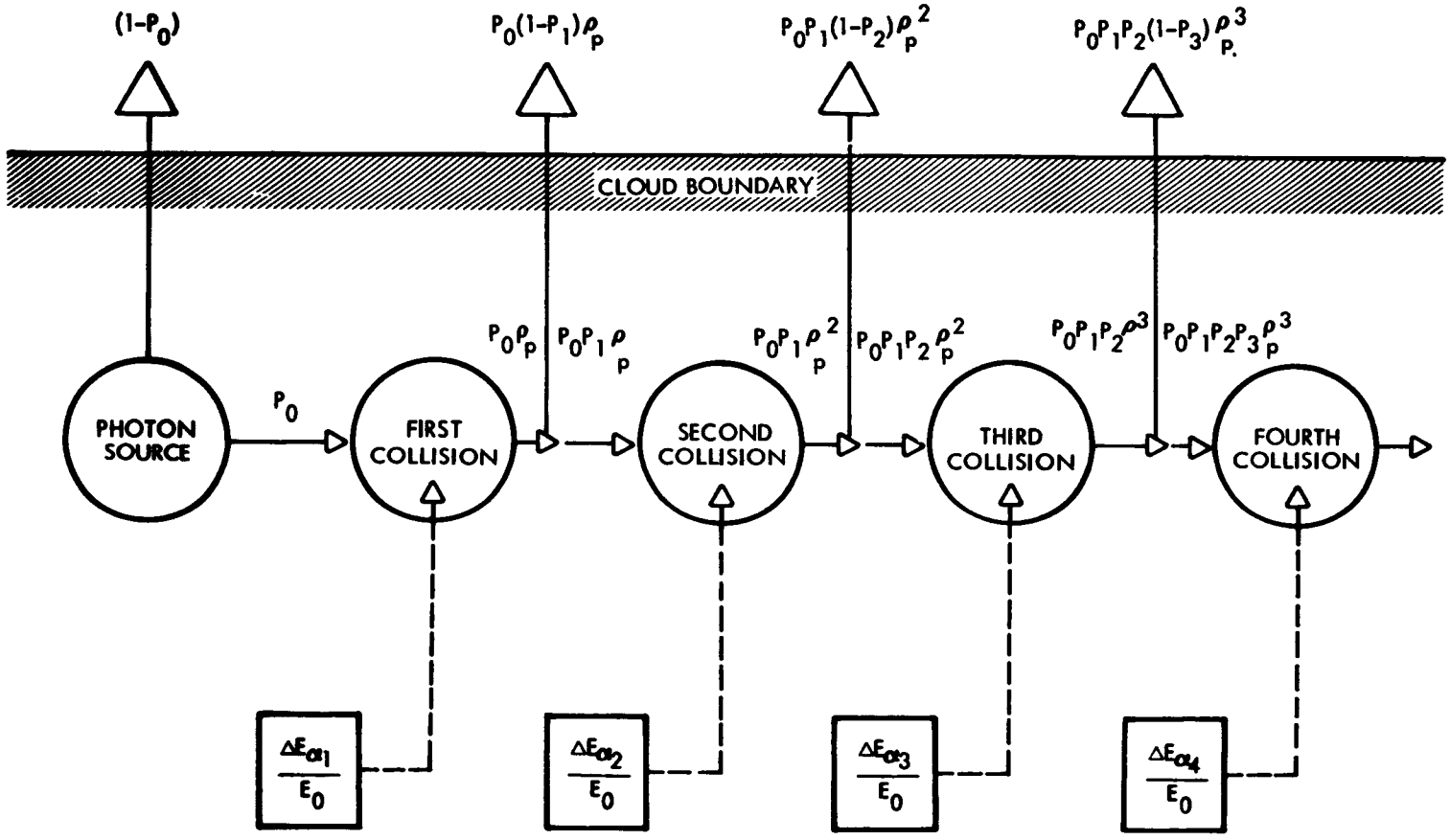

Figure 2. Probability of Photon Absorption in a Particle Cloud

The total energy absorbed by particles through collisions is then

$$E_a = \sum_{i=1}^{\infty} \Delta E_{a_i} = E_o(1 - \rho_p)\left[P_o + P_o P_1 \rho_p + \cdots + P_o P_1 P_2 \cdots P_n \rho_p^{\,n} + \cdots\right] = E_o(1 - \rho_p) \sum_{j=1}^{\infty} \rho_p^{j-1} \prod_{i=1}^{j} P_{i-1}$$

The absorptivity or emissivity of the particle cloud is the ratio of the total absorbed energy to the total incident energy, which is defined as

$$\alpha_a = \epsilon_a = \left(\frac{E_a}{E_o}\right) = (1 - \rho_p) \sum_{j=1}^{\infty} \rho_p^{j-1} \prod_{i=1}^{j} P_{i-1} \tag{3}$$

Equation (3) can be simplified by assuming that the particles are opaque, i.e., $\rho_p = (1 - \epsilon_p)$. Thus

$$\epsilon_a = \epsilon_p \sum_{j=1}^{\infty} (1 - \epsilon_p)^{j-1} \prod_{i=1}^{j} P_{i-1} \tag{4}$$

A comparison of Equation (4) with (2) shows an analogy between neutron blackness and apparent emissivity.

For both neutrons and photons, the change of intensity due to absorption and scattering is a function of particle total cross section and particle concentration. The total cross section is a measure of the energy taken away by an individual particle and consists of absorbing and scattering cross sections ($\sigma_t = \sigma_s + \sigma_a$). It is seen from Equations (2) and (4) that the ratios of the neutron absorption and scattering cross sections to the total cross section, (σ_a/σ_t) and (σ_s/σ_t) are equivalent to the absorptivity and reflectivity, ϵ_p and $1 - \epsilon_p$, respectively, of a particle in the radiating medium.

The above expression can be applied to any cloud geometry. The effects of the cloud shape, the total cross section, and the particle concentration are reflected in each of the probability functions $P_{i-1,k}$.

2. Probability Functions

The determination of the first few probability functions is shown below for an infinite slab of particles. Consider a beam of

rays traversing a slab in the direction of θ with respect to a line perpendicular to the slab (Figure 3). Take an element of this beam of length dx and cross section A at x distance from the boundary. The total number of particles in this element is NA dx and the total cross section of these particles is σ_t NA dx. Then the fraction of energy removed in the element through absorption and scattering is

$$\left(\frac{N\sigma_t A\, dx}{A}\right) = N\sigma_t\, dx$$

The rate of change of the intensity of radiant energy may be determined as follows

$$I + \left(\frac{\partial I}{\partial x}\right) dx = I - (N\sigma_t\, dx)\, I$$

$$\left(\frac{\partial I}{\partial x}\right) = -(N\sigma_t)\, I \tag{5}$$

Integrating this once

$$I = I_o\, e^{-N\sigma_t x} \tag{6}$$

where I_o is intensity at $x = 0$.

If the usual cosine function distribution of the radiant energy intensity is assumed for entrant distribution, then the initial intensity I_o may be defined in terms of a maximum intensity as a function of the cosine of directional angle θ.

$$I_o = I_m(\cos\theta)^k = I_m\mu^k$$

Substituting this expression into Equation (6)

$$I = I_m\mu^k\, e^{-N\sigma_t x} \tag{7}$$

Differentiating the above equation

$$\left(\frac{\partial I}{\partial x}\right) = -N\sigma_t I_m\mu^k\, e^{-N\sigma_t x} \tag{8}$$

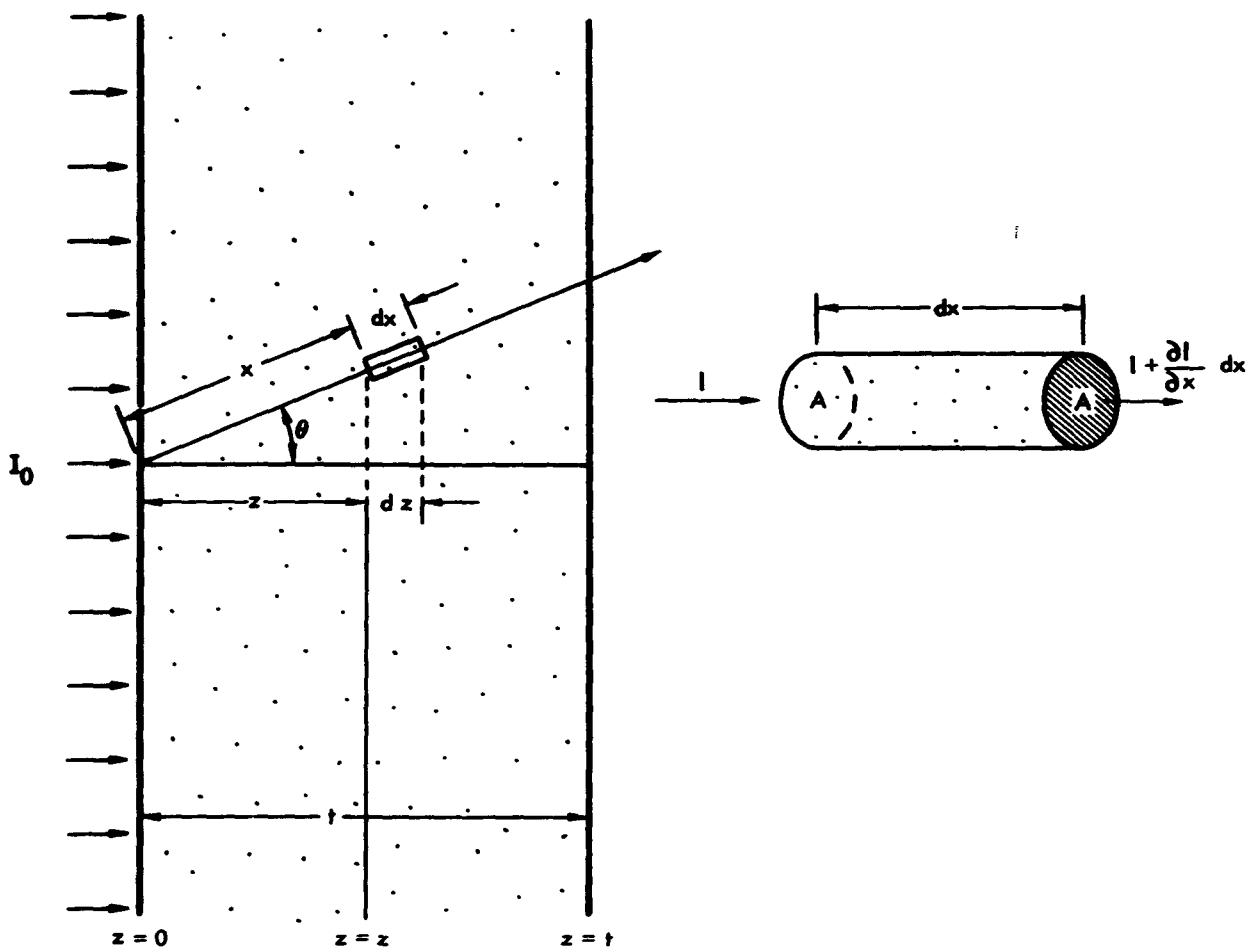

Figure 3. Particle Cloud Geometry

The energy loss per unit length along a path may be defined as

$$\frac{dE}{dx} = -2\pi \left(\frac{\partial I}{\partial x}\right) d\mu$$

Combining this equation with Equation (8)

$$\left|dE\right| = -2\pi I_m N\sigma_t \mu^k e^{-N\sigma_t x} \, d\mu \, dx$$

The total energy loss for a plane wave traversing across the slab of thickness, t, is then determined by integrating the above differential equation over the slab thickness, t, and the solid angle 2π steradians as follows

$$E_t = 2\pi I_m \int_o^t N\sigma_t \int_o^1 \mu^{k-1} e^{-N\sigma_t z/\mu} \, d\mu \, dz \tag{9}$$

The total energy incident to the slab can be determined as

$$E_o = 2\pi \int_o^1 I_o \, d\mu = 2\pi I_m \int_o^1 \mu^k \, d\mu = \frac{2\pi I_m}{(k+1)} \tag{10}$$

The probability of photons colliding with particles on their first flight in the slab is

$$P_{o,k} = \left(\frac{E_t}{E_o}\right) = (k+1) \int_o^t N\sigma_t \int_o^1 \mu^{k-1} \, e^{-N\sigma_t z/\mu} \, d\mu \, dz \tag{11}$$

As shown by the above integral, the probability function is dependent on the particle concentration, total cross section, and the cloud geometry.

In order to determine the second collision probability, the probability that photons reflected isotropically by a particle at a distance, z, escape through the surface z = t without suffering further collision must be defined first. (This probability is denoted by P(z).) If the intensity of the radiant energy reflected isotropically at z = z is denoted by I_s, then the intensity of the energy transmitted from z = z to the surface z = t in the direction of θ may be expressed as

$$I_{tr} = I_s e^{-N\sigma_t(t - z)/\mu}$$

The total energy transmitted from z = z to z = t is then determined as

$$E_{tr} = 2\pi \int_o^1 I_{tr}\, d\mu = 2\pi I_s \int_o^1 e^{-N\sigma_t(t - z)/\mu}\, d\mu \qquad (12)$$

and the total energy scattered at z = z toward the surface z = t is

$$E_s = 2\pi \int_o^1 I_s\, d\mu = 2\pi I_s \qquad (13)$$

Thus

$$P(z) = \frac{1}{2}\left(\frac{E_{tr}}{E_s}\right) = \frac{1}{2}\int_o^1 e^{-N\sigma_t(t - z)/\mu}\, d\mu \qquad (14)$$

where the factor of 1/2 accounts for the half space.

Similarly, the probability that photons reflected isotropically at z = z escape through the surface z = 0 can be defined as

$$P'(z) = \frac{1}{2}\int_o^1 e^{-N\sigma_t z/\mu}\, d\mu \qquad (15)$$

Hence, the probability that once scattered photons escape through the surfaces z = 0 and z = t is

$$P_{o,k}(1 - P_{1,k})\rho_p = \rho_p(k + 1)\int_o^t N\sigma_t \left[P(z) + P'(z)\right]\int_o^1 \mu^{k-1} e^{-N\sigma_t z/\mu}\, d\mu\, dz$$

The second collision probability, therefore, is

$$P_{1,k} = 1 - \frac{(k+1)}{P_{o,k}}\int_o^t N\sigma_t\left[P(z) + P'(z)\right] \int_o^1 \mu^{k-1} e^{-N\sigma_t z/\mu}\, d\mu\, dz \qquad (16)$$

By successive generations of the probability functions, the third collision probability can be similarly determined as

$$P_{2,k} = 1 - \left(\frac{N\sigma_t}{2}\right)^2 \frac{(k+1)}{P_{o,k} \cdot P_{1,k}} \int_o^t \left[P(z) + P'(z)\right] \int_o^t \int_o^1 \mu^{k-1} e^{-N\sigma_t z'/\mu} d\mu$$

$$\int_o^1 \mu^{-1} e^{-N\sigma_t(z-z')/\mu} d\mu\, dz'\, dz \qquad (17)$$

The equations for the collision probability can be simplified by using the integroexponential functions, the values of which are readily available. The function is

$$\tilde{E}_i(\phi) = \int_o^1 \mu^{i-2} e^{-\phi/\mu} d\mu \qquad (18)$$

Thus, Equations (11), (16), and (17) become

$$P_{o,k} = (k+1) \int_o^t N\sigma_t \tilde{E}_{k+1}(N\sigma_t z)\, dz \qquad (19)$$

$$P_{1,k} = 1 - \frac{(k+1)}{2P_{o,k}} \int_o^t N\sigma_t \tilde{E}_{k+1}(N\sigma_t z) \left[\tilde{E}_2(N\sigma_t z) + \tilde{E}_2(N\sigma_t t - N\sigma_t z)\right] dz \qquad (20)$$

$$P_{2,k} = 1 - \left(\frac{N\sigma_t}{2}\right)^2 \frac{(k+1)}{P_{o,k} \cdot P_{1,k}} \int_o^t \left[\tilde{E}_2(N\sigma_t z) + \tilde{E}_2(N\sigma_t t - N\sigma_t z)\right]$$

$$\int_o^t \tilde{E}_{k+1}(N\sigma_t z') \tilde{E}_1(N\sigma_t z - N\sigma_t z')\, dz'\, dz \qquad (21)$$

It is apparent from the above equations that the collision probability is a function of $(N\sigma_t t)$ and k. The first parameter $(N\sigma_t t)$ is called "optical thickness" and is a product of particle concentration, total (extinction) cross section and slab thickness. The second parameter is the exponent of the cosine function which represents the entrant distribution of radiant energy. If an isotropic emission is assumed, k = 0 is used.

3. Variation of Apparent Emissivity with Optical Thickness and Particle Emissivity

Using the foregoing approach, Anthony and Stuart, respectively, developed the neutron blackness curves for the infinite slab and cylinder in connection with their neutron diffusion studies. The optical equivalent of these curves is presented in Figure 4. The apparent emissivity for a constant particle emissivity is a monotonically increasing function of optical thickness, τ. For large values of τ (optically thick cloud), the emissivity curves approach asymptotically a limiting value, regardless of the cloud geometry. For very small values of τ, however, the apparent emissivity differs for different geometry. For very small values of τ, a linearization of the apparent emissivity function results in the following approximations.

$$\epsilon_a = 1\epsilon_p \tau \qquad \text{for a cylinder}$$

$$\epsilon_a = 2\epsilon_p \tau \qquad \text{for a slab}$$

It is observed that the emissivity for a slab increases (with τ and ϵ_p) twice as fast as that for a cylinder in the region of very small τ.

Although the configuration of a rocket exhaust particle plume resembles a cone, the emissivity for the cylindrical configuration is used here because the values of the probability functions for a cone are analytically intractable and because the axial symmetry of the cylinder approximates reasonably well the rocket plume geometry.

4. Optical Thickness and Particle Emissivity

It has been shown that the apparent emissivity for particle clouds is a function of particle emissivity and optical thickness. Therefore, if these quantities are known for a given cloud of radiating particles, then the neutron blackness curves developed for a similar geometry may be used to determine the apparent emissivity for the particle cloud.

a. Optical Thickness

The optical thickness for a cloud of particles of uniform size and uniform concentration is defined as

$$\tau = N\sigma_t \ell$$

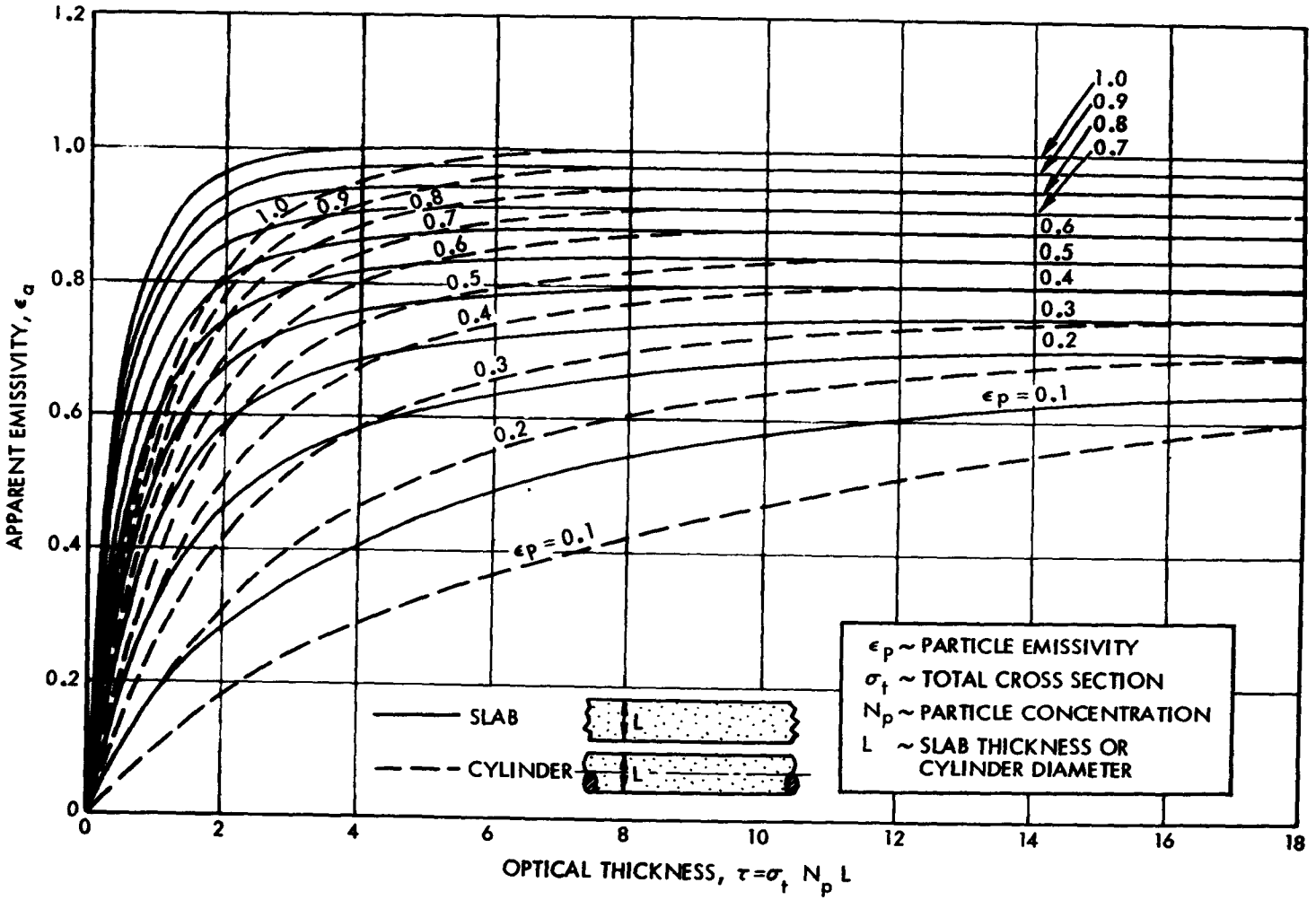

Figure 4. Apparent Emissivity for a Cloud of Particles in the Form of a Slab or a Cylinder

Inasmuch as the particle plume for a typical aluminized propellant rocket consists of varying size particles and, furthermore, the particle concentration is not uniform in the flow field, the optical thickness cannot be determined directly by use of the above expression. In computation of the particle plume flow field by the computer program,[2] five distinct particle sizes were used to simulate the actual flow field. Consequently, a superposition technique which sums up the thicknesses for all particle sizes has been adopted. The equation is

$$\tau = \sum_{n=1}^{5} \sigma_{t_n} \int_{o}^{\ell_n} N_n(x)\, dx \tag{22}$$

The total cross section, σ_t, of a particle plume may be expressed in terms of the particle geometrical cross section as

$$\sigma_t = Q_t \pi r_p^2 \tag{23}$$

The coefficient Q_t is called "extinction efficiency factor" and is discussed quite extensively in References 6 and 7. This efficiency factor is a function of the particle size and shape, the refractive indices of the materials involved, and the radiation wavelength. The values of the total cross section for small carbon particles determined by the Mie theory are presented in Reference 8. For sapphire,* values are given in Reference 9.

According to the Mie theory, the extinction efficiency factor of a particle can be expressed as a function of

$$a = \left(\frac{2\pi r_p}{\lambda}\right)$$

As this value increases, the value of Q_t also increases for small values of a. If the imaginary part of the refractive index is of a small order of magnitude (small absorption coefficient), Q_t oscillates for intermediate values of a. However, for large values of a, the oscillation damps out and the value of Q_t becomes equal to 2. This fact is shown in Reference 6 for numerous materials.

*Aluminum oxide of single or few crystals

The value of a for the particle plumes under consideration is greater than 6 since the mean particle diameter is 4 microns and the wavelength for maximum radiant power is from 1.5 to 2.0 microns. For this value of a, the efficiency factor may be assumed to be 2. Thus, the total cross section σ_t in Equation (22) is taken as twice the geometric cross section of the spherical particles.

b. Particle Emissivity

As can be seen from Figure 4, the particle emissivity is equally as important as τ in determining the apparent emissivity of a particle cloud. A theoretical approach to the determination of particle emissivity is to apply the Mie theory to a sphere of appropriate size and observe the values of

$$\epsilon_{p_\lambda} = \left(\frac{\sigma_{a_\lambda}}{\sigma_{t_\lambda}}\right) = \left(\frac{Q_{a_\lambda}}{Q_{t_\lambda}}\right)$$

from which a total emissivity, ϵ_p, can be obtained. The values of Q_{a_λ} and Q_{t_λ} given in Reference 9 for aluminum oxide (sapphire) result in a value of ϵ_p considerably less than 0.1. Higher values of particle emissivity determined grossly from measurements of rocket exhausts are in conflict with this result. It is suspected that the optical properties for sapphire, upon which the calculations of Reference 9 were based, are not representative of those for aluminum oxide particles in rocket exhausts. One argument which has been advanced is that the absorptive properties of the particles are higher than those of sapphire, due to a polycrystalline-porous structure of the former. Lee and Kingery[10] have explored this argument in some detail. The high experimental values of particle emissivity seem to justify the assumption of opaqueness in Equation (4).

For application to the present problem, a single value of $\epsilon_p = 0.25$ was chosen. This value was determined based on extrapolation of bulk aluminum oxide emissivity measurements. The single value is justified because of the small sensitivity of particle emissivity to temperature in the range of the temperature of the particles. The values presented and discussed in Section III tend to confirm the choice of $\epsilon_p = 0.25$.

The mechanics used to arrive at the particle emissivity from rocket plume measurements were as follows: Narrow angle radiometer measurements yielding $\dot{q}$ were made viewing across the exhaust plume near the nozzle exit. (The particle flow field is known most accurately at this location in the exhaust.) An average particle temperature along the line of view was determined as described below. The equation

$$\dot{q} = \overline{\epsilon}_a \sigma_b \overline{T}^4 \tag{24}$$

was then solved for $\overline{\epsilon}_a$. The value of τ along the line of view was determined as described above. The effective particle emissivity was then determined by use of the cylinder curves of Figure 4.

5. Specific Values of Apparent Emissivity

With the value of τ determined for any desired view through the axis of the particle plume, and with the value of ϵ_p determined as described above, Figure 4 can be used to obtain $\overline{\epsilon}_a$ for the plume segment encompassing that view.

Each segment of the rocket plume is treated as a cylindrical particle cloud whose axis is normal to the view line from the surface element through the center of that segment. The value of τ_i is computed based on the length of that view line, ℓ_n, per Equation (22). This value of τ_i along with ϵ_p are used with the curves given in Figure 4 for a cylindrical cloud to obtain a value of ϵ_{a_i} for the plume segment. The value of ϵ_{a_i} so derived is taken to be $\overline{\epsilon}_{a_i}$ for the segment surface since the value of ϵ_a taken through the diameter of a cloud cylinder represents a mean value for that cylinder.[11]

B. EFFECTIVE PLUME TEMPERATURE

The particle temperature of an exhaust plume varies with particle size and particle location. Hence, an average temperature of particles along a given path is required to determine the heat rate from these particles. Since heat rates measured by narrow angle radiometers are restricted to a small field of view of a cone about the instrument axis, an average temperature of particles along this axis will suffice to determine the heat rate to the instrument. However, for calorimeter measurements, the field of

view is hemispherical (solid angle of 2π steradians). Therefore, to determine a heat rate to a calorimeter, the temperature variations of the plume in lateral as well as longitudinal directions should be considered. The longitudinal variation is accounted for by segmenting the plume into a number of slices. However, the lateral variation is accounted for by applying an averaging correction factor to the average temperature of particles along a pencil view through the centerline.

Consequently, determination of the particle plume temperature is reduced to computing the average particle temperature along a given line through the plume axis. Inasmuch as a heat rate from a particle cloud to a given point is proportional to particle temperature to the fourth power, to particle concentration, particle cross section, and cloud thickness, and is inversely proportional to the square of distance between the point of interest and an individual particle, the following averaging technique accounting for all these effects has been used to determine the effective temperature,

$$\bar{T} = \left[\eta \frac{\int_{L_o}^{L_o+L} \sum_{n=1}^{5} N_n r_{p_n}^2 T_{p_n}^4 \frac{dx}{x^2}}{\int_{L_o}^{L_o+L} \sum_{n=1}^{5} N_n r_{p_n}^2 \frac{dx}{x^2}} \right]^{1/4} \tag{25}$$

The correction factor η is determined by taking the temperature variation in a lateral plane of view and averaging it over all view lines contained in that plane weighted by lateral variation of shape factor.

C. TOTAL RADIATION FROM PARTICLE PLUME

To determine a total heat flux from the particle plume to a given surface element, a heat flux from an infinitesimal slice of the plume must be integrated over the visible region of the plume. The integral equation defining the total heat flux is

$$\dot{q} = \int_{\gamma_o}^{\gamma_1} \epsilon_a\left(r(\gamma)\right)\sigma_b \bar{T}^4(\gamma) \left(\frac{dF}{d\gamma}\right) d\gamma \tag{26}$$

The above integration may be performed numerically by segmenting the unshaded portion of the plume with a number of path planes extending from the surface element to the plume, as shown in Figure 1. For each of these segments, the mean values of optical thickness, τ_i, apparent emissivity, $\bar{\epsilon}_a$, and effective temperature, $\bar{T}_i$, can be determined. Shape factors, ΔF_i, from the surface element to these segments can also be determined by use of an available analytical technique.[1] Then, the total heat flux from the plume is determined as

$$\dot{q} = \sigma_b \sum_{i=1}^{m} \bar{\epsilon}_{a_i}(\tau_i) \bar{T}_i^4 \Delta F_i \qquad (27)$$

III. ANALYTICAL PREDICTIONS AND EXPERIMENTS

A. DESCRIPTION OF EXPERIMENTAL TESTS

1. Test Models and Environment

Experimental data were taken during the firing of two aluminized propellant rockets under simulated pressure altitude conditions. One rocket, the smaller (A), exhausted through a contoured nozzle of expansion ratio 19:1 which had an exit diameter of approximately 12 inches. The second rocket (B) exhausted from a somewhat similar nozzle of expansion ratio 23.5:1 and exit diameter about 26 inches. The chamber temperatures and the percentages of aluminum oxide in the exhausts were representative of those for typical aluminized propellants.

The firings were made in a test cell arrangement which employed a diffuser and an auxiliary pumping system, as shown schematically in Figure 5. Average pressure altitudes of 110,000 feet and 130,000 feet were maintained during rocket (A) and rocket (B) firings, respectively. These altitudes were sufficiently high to permit expansion of the particle plume into as large a plume immediately downstream of the nozzle exits as would occur in a near vacuum. The recirculatory gas flow from the boundary of the exhaust gas plume was scavenged by the auxiliary pump, permitting only a small amount of convective heating in the area at and upstream of the nozzle exit.

2. Particle Flow Field

A particle flow field was developed for the condition of each of the two rockets exhausting into a near vacuum ($p_c/p_e = 10^5$) by the computer program of Reference 2. In each case the particle size distribution was taken to be:

Particle Number	Radius, (microns)	Percent of Total Al_2O_3
1	0.79	20
2	1.28	20
3	1.76	20
4	2.44	20
5	3.95	20

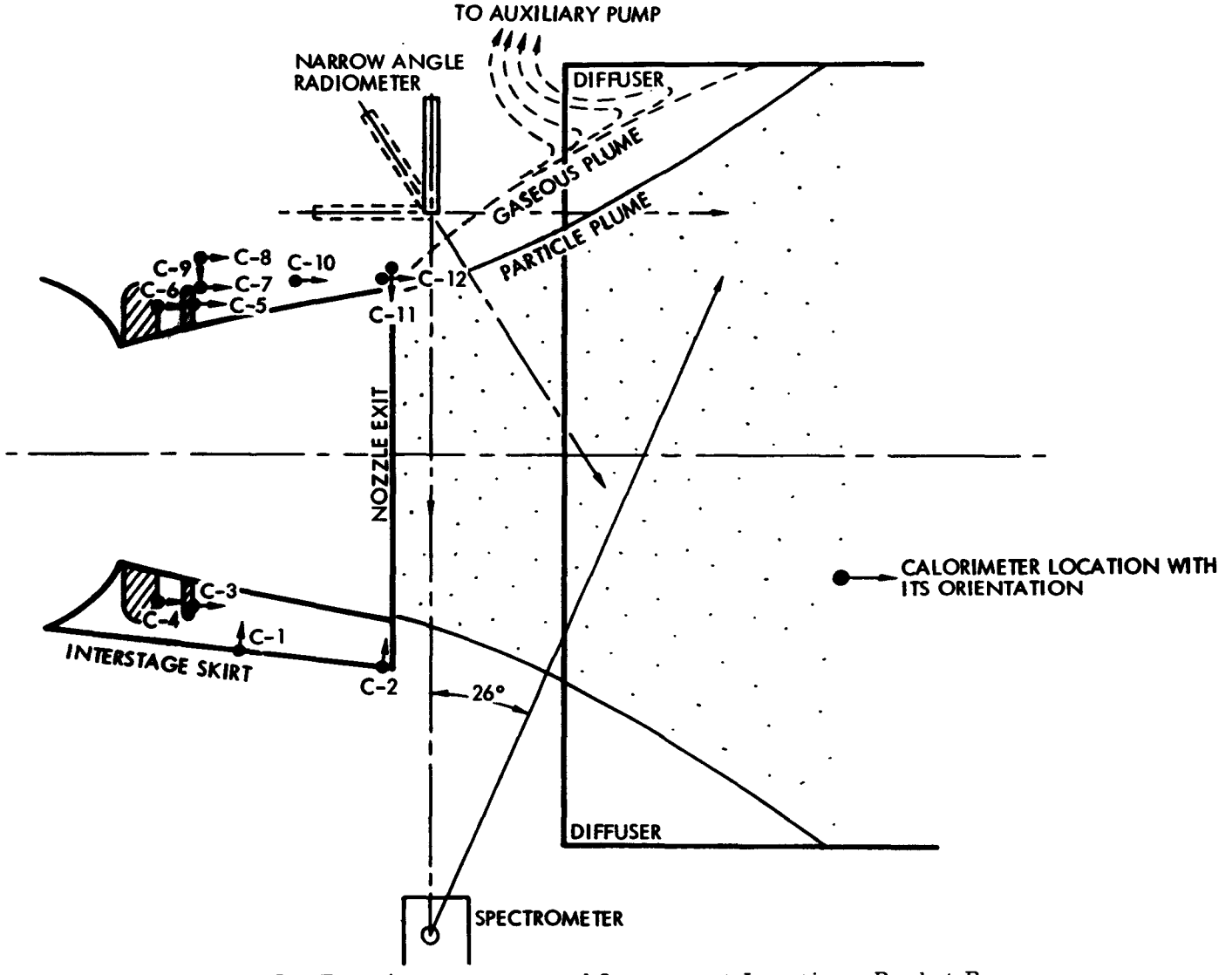

Figure 5. Test Arrangement and Instrument Locations-Rocket B

This distribution,[12] based on samples collected on glass slides during simulated firings of rockets containing similar propellant, results in a mean particle radius of 2.04 microns. Sample flow field information for the two extreme particle sizes are shown for rocket (B) in Figures 6 and 7.

3. Instrumentation

Instrumentation for measurement of thermal radiation was of three types: (1) narrow angle (5 degrees solid angle) radiometers, (2) black surfaced asymptotic calorimeters, and (3) spectrometers which scanned the wave length range 0.3 to 4.5 microns. Data used from the rocket (A) firing was taken by narrow angle radiometers which viewed across the particle plume 3 inches downstream of the nozzle exit and normal to the plume axial centerline. Data taken from the rocket (B) firing employed all three types of instruments. Figure 5 indicates the instrument locations for rocket (B).

B. EXPERIMENTAL RESULTS AND COMPARISON WITH ANALYTICAL PREDICTIONS

1. Aluminum Oxide Particle Emissivity

The aluminum oxide particle emissivity was determined as described in Section II from 5 radiometer measurements from the rocket (A) plume and from 7 similar measurements from rocket (B). Values are plotted in Figure 8 along with emissivity measurements made on bulk alumina[13] at elevated temperatures. The reasonably good agreement between the two suggests that the particle emissivity approaches that of the bulk material rather than the low values of sapphire. This seems to corroborate the explanations given by Lee and Kingery[10] and Kuby and Carlson.[14] A value of particle emissivity was also determined by integrating the measured spectral intensities over wavelength and dividing by the integrated black body intensity. This value, $\epsilon_p = 0.3$, tends to confirm the radiometer measurements.

It is seen from the spectral intensity data (Figure 9) that the plume radiation intensity decreases on either side of the peak wavelength at a rate faster than that of black (or gray) body. Thus, while the plume of rocket (B) radiates in a manner somewhat similar to a gray body, it cannot be considered a gray body.

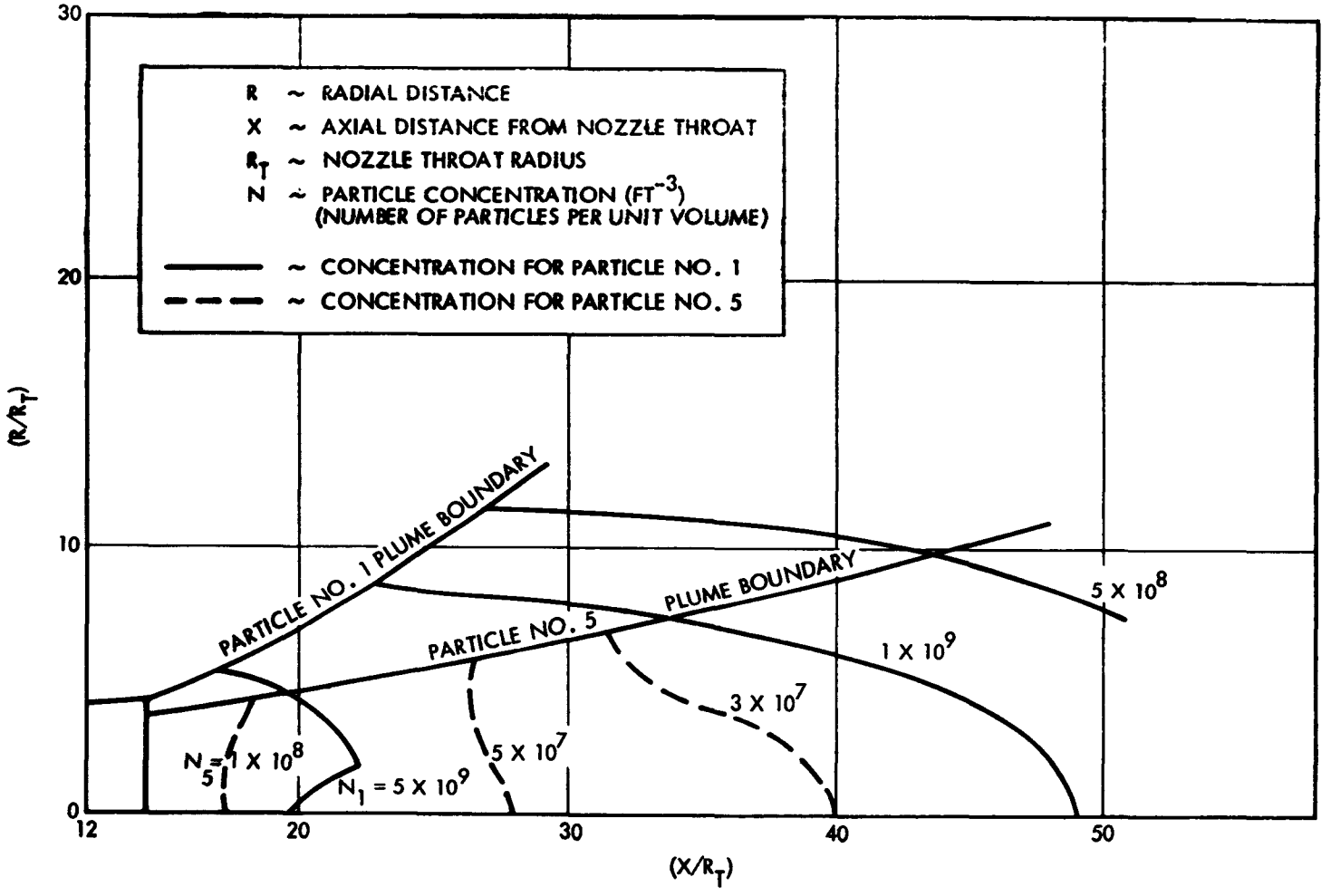

Figure 6. Particle Concentration Distribution

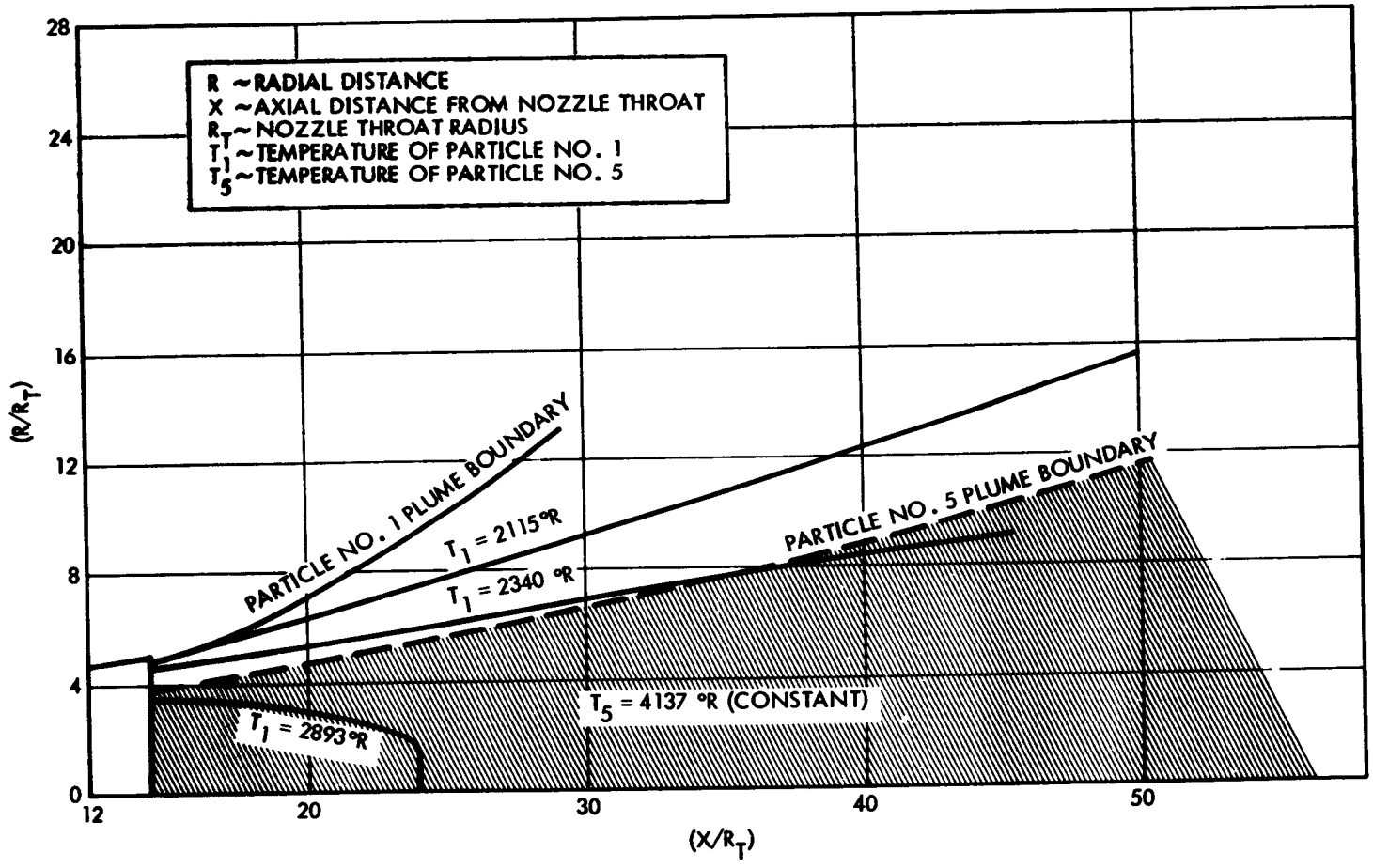

Figure 7. Particle Temperature Distribution

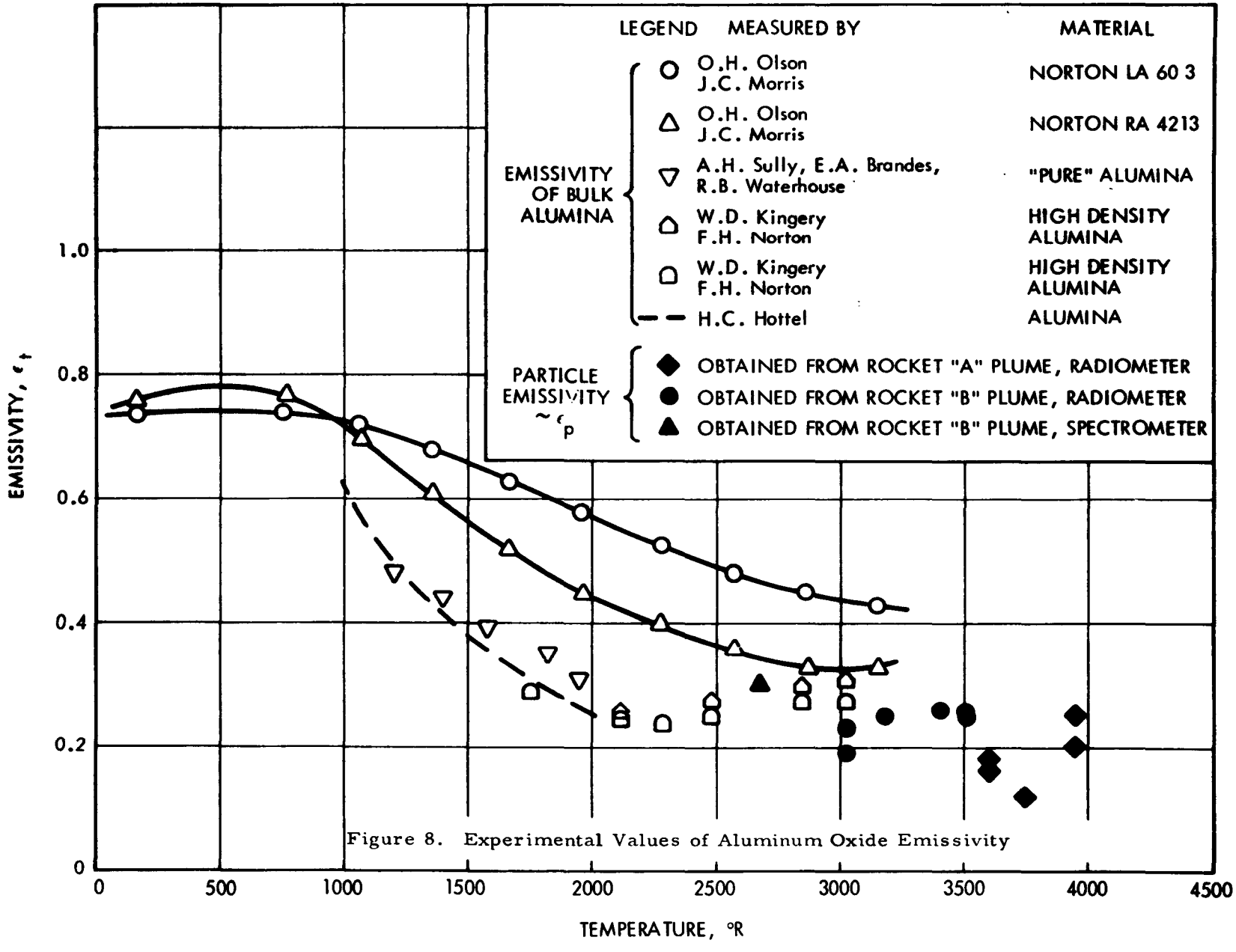

Figure 8. Experimental Values of Aluminum Oxide Emissivity

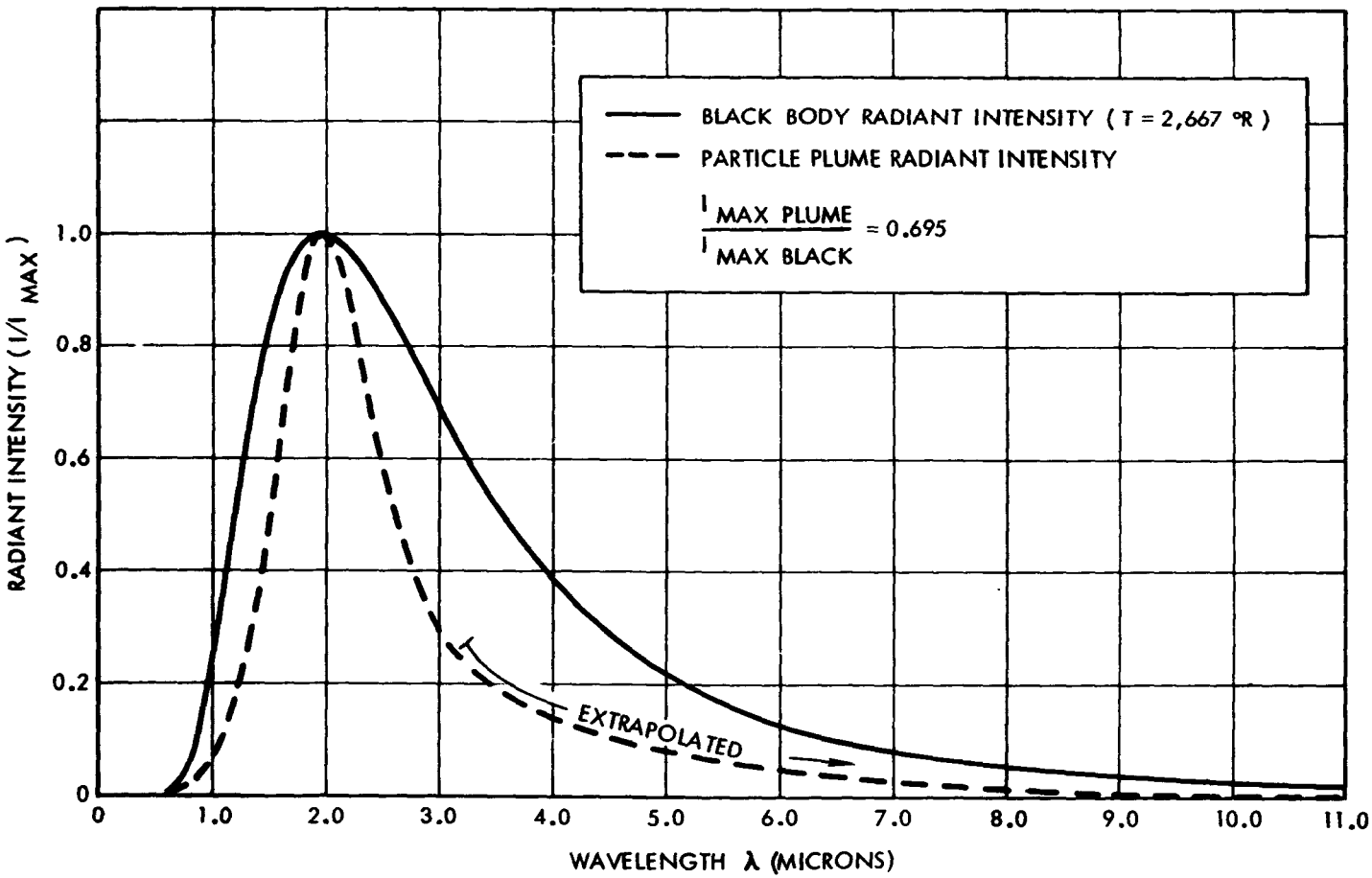

Figure 9. Radiant Intensity Spectral Distribution

2. Heat Rates to Surface Elements

Using the method developed in Section II, the particle flow field for rocket (B), and a particle emissivity of 0.25, predictions were made of heat rates from the particle plume of the larger rocket to the calorimeters (surface elements) located as shown in Figure 5. The effect of the presence of the diffuser was taken into account approximately in the following manner. The particle concentrations were assumed to remain constant downstream of the point at which the theoretical particle limiting trajectories intersect the diffuser wall. The concentrations were taken to be equal to those in the plane of that intersection. For purposes of determining τ and $\overline{T}$ for those segments which extend downstream along the length of the diffuser, the particle plume (constrained by the diffuser) was cut off at three nozzle exit diameters downstream of the nozzle exit, since downstream of this point, the values of $\overline{T}$ and τ (and therefore $\overline{\epsilon_a}$) would increase such a small amount that their effect on the contribution to $\dot{q}$ to the surface element from that segment is negligible.

Table 1 compares the predictions with experimental values measured during the firing of rocket (B). The agreement is considered quite good for engineering predictions of heat rates.

Table 1. Comparison of Predictions With Experimental Results

Calorimeter	$\dot{q}_{Prediction}$	$\dot{q}_{Test}$	$\frac{(\dot{q}_{Prediction}-\dot{q}_{Test})}{\dot{q}_{Test}}$
C-1	0.67	0.54	+0.241
C-2	7.00	5.78	+0.211
C-3	1.10	1.03	+0.068
C-4	1.05	0.83	+0.265
C-5	1.05	1.13	-0.071
C-6	1.12	1.03	+0.087
C-7	1.36	1.39	-0.022
C-8	1.76	2.12	-0.170
C-9	0.35	0.32	+0.094
C-10	2.50	3.10	-0.194
C-11	9.40	12.07	-0.221
C-12	5.00	8.35	-0.401

Arithmetic Mean of Absolute Values of Deviation Between Test Data and Prediction

$$\frac{\Delta\dot{q}}{\dot{q}} = 0.17$$

The relatively large differences between predictions and experiment experienced on calorimeters 11 and 12 deserve further comment. It is believed that convective heating due to recirculation of hot gas inside the test cell, aluminum oxide slag protruding from the nozzle wall at its exit, and reflection from the supporting bracketry combined to increase the measured values. These effects have not been accounted for in the analytical predictions. Including these two measurements, the average difference between predictions and experimental values is 17 percent of the latter. If these two measurements are ignored, this value is reduced to 14.2 percent.

C. APPLICATION OF ANALYTICAL METHOD

It is the opinion of the authors that the method developed here can be used to predict radiant heat rates incident to surfaces located in the region surrounding the plume of a wide range of particle laden rocket exhausts. Examples are temperature sensitive spacecraft surfaces and rocket aft closures and components located near the exhaust. Requirements are that the particle radiation level be so large compared to that of the gas that the latter is negligible and that the particle material and size distribution be known with sufficient accuracy to permit development of the flow field by means of a two-phase flow computer program. The particle emissivity must also be known.

Predictions should be suitably accurate for design purposes except possibly for cases in which the surface elements are oriented such that they view only a small sector along the outer edges of the exhaust plume. An example of these surface elements is the outer surface of the nozzle wall (Figure 1).

It seems clear that, in this instance, the approximation of a plume segment by a cylindrical particle cloud is not valid. Fortunately, the heat rates from the plume to surface elements so located are small and are usually not of major concern.

IV. CONCLUSIONS

An approximate method has been developed which analytically predicts radiant heat rates incident to adjacent surfaces produced by a rocket exhaust containing a large percentage of its mass flow as aluminum oxide particles and operating in a rarefield atmosphere. Predictions can be made with accuracies suitable for engineering design.

The emissivity of aluminum oxide particles in a rocket exhaust appears to be between 0.1 and 0.3 and is not inconsistent with extrapolated data for bulk alumina at a temperature in the vicinity of $3500^{\circ}R$.

An aluminum oxide particle plume radiates in a manner somewhat similar to a gray body. For wavelengths on either side of that at which the intensity peaks, the rate of intensity decay is considerably greater than that of a gray body.

REFERENCES

1. S.J. Morizumi, "Analytical Method of Determining Shape Factor From a Surface Element to a Conical Surface," Space Technology Laboratories, Inc., Redondo Beach, California, internal memorandum 62-9721.4-78; October 1962.

2. G.R. Nickerson and J.R. Kliegel, "The Calculation of Supersonic Gas-Particle Flows in Axi-symmetric Nozzles by the Method of Characteristics," Space Technology Laboratories, Inc., Redondo Beach, California, Report 6120-8345-MU000; May 1962.

3. G.W. Stewart, "Multiple Scattering of Neutrons," Nuclear Sci. and Eng. 2, pp. 617-625; 1957.

4. G.W. Stewart and R.W. Woodruff, "Method of Successive Generations," Nuclear Sci. and Eng. 3, 339-373; 1958.

5. G.W. Anthony, "The Average Escape Probabilities for Once and Many-Times Scattered Neutrons for a Slab," General Electric Co., Hanford Atomic Products Operations Report HW-49188; March 1957.

6. H.C. Van de Hulst, Light Scattering by Small Particles, John Wiley and Sons, Inc., New York, 1957; Chap. VIII, p. 107.

7. J.A. Stratton, Electromagnetic Theory, McGraw-Hill Book Co., Inc. New York, 1941; Chap. IX, p. 569.

8. V.R. Stull and G.N. Plass, "Emissivity of Dispersed Carbon Particles," J. Opt. Soc. Am., pp. 121-129; February 1960.

9. G.N. Plass, "Mie Scattering and Absorption Cross Sections of Aluminum-Oxide and Magnesium-Oxide," Aeronutronic Division of Philco Corp.; Final Report SSD-TDR-62-127-V6; May 1963.

10. D.W. Lee and W.D. Kingery, "Radiation Energy Transfer and Thermal Conductivity of Ceramic Oxides," J. Am. Ceram. Soc. 43, 594-606; 1960.

11. W.H. McAdams, Heat Transmission, McGraw-Hill Book Company, Inc., New York, 1964, 3rd ed., Chap. IV, p. 88, 105.

12. J.R. Kliegel, "Gas Particle Nozzle Flows," Ninth International Symposium on Combustion, Combustion Institute, Academic Press, New York, 1963; pp. 811-826.

13. A. Goldsmith, T.W. Waterman and H.J. Hirschborn, Handbook of Thermophysical Properties of Solid Materials, The MacMillian Co., New York, 1961; Vol. 3, Chapter VII, p. 43.

14. D. Carlson and W. Kuby, "An Investigation of Recombination and Particle Lag Effects in Rocket Nozzles (U)," Fifth Quarterly Technical Summary Report, Aeronutronic Division, Philco, Publication No. C-2265, September 1963. (C)

DISTRIBUTION

R. C. Anderson
W. J. Bauchwitz (5)
C. W. Besserer
J. T. Bevans
R. Bromberg
J. R. Burnett
J. A. Champion (5)
C. B. Cohen
J. O. Crum
K. L. Goldman
R. O. Gose
A. F. Grant, Jr.
D. E. Kennedy
J. R. Kliegel
H. P. Liepman
R. P. Lipkis
J. T. Ohrenberger
E. C. Rea (5)
J. R. Sellars
I. N. Spielberg
W. R. Wannlund
I. Zuckerman

STL Technical Library
(2 + 1 reproducible)

DDC (20)

AF Contracting Officer (1)

UNCLASSIFIED

TRW Space Technology Laboratories Inc., One Space Park · Redondo Beach, California
THERMAL RADIATION FROM THE EXHAUST PLUME OF AN ALUMINIZED COMPOSITE PROPELLANT ROCKET, by S.J. Morizumi and H.J. Carpenter. January 1964. 37 p. incl. illus. (6121-7904-RU-000; BSD-TDR-64-16)
(Contract AF 04(694)-1) Unclassified report

A technique is developed for calculating rocket base heating and spacecraft heating environments due to particle radiation from a single nozzle rocket exhaust plume. The technique has proved successful when applied to a single nozzle exhausting into a rarefied atmosphere on the basis of comparison of predictions with experimental results.

The analysis treats radiation from a cloud of particles as that from an equivalent radiating surface. Thus, the problem is reduced to the
(over)

UNCLASSIFIED

UNCLASSIFIED

TRW Space Technology Laboratories Inc., One Space Park · Redondo Beach, California
THERMAL RADIATION FROM THE EXHAUST PLUME OF AN ALUMINIZED COMPOSITE PROPELLANT ROCKET, by S.J. Morizumi and H.J. Carpenter. January 1964. 37 p. incl. illus. (6121-7904-RU-000; BSD-TDR-64-16)
(Contract AF 04(694)-1) Unclassified report

A technique is developed for calculating rocket base heating and spacecraft heating environments due to particle radiation from a single nozzle rocket exhaust plume. The technique has proved successful when applied to a single nozzle exhausting into a rarefied atmosphere on the basis of comparison of predictions with experimental results.

The analysis treats radiation from a cloud of particles as that from an equivalent radiating surface. Thus, the problem is reduced to the
(over)

UNCLASSIFIED

UNCLASSIFIED

TRW Space Technology Laboratories Inc., One Space Park · Redondo Beach, California
THERMAL RADIATION FROM THE EXHAUST PLUME OF AN ALUMINIZED COMPOSITE PROPELLANT ROCKET, by S.J. Morizumi and H.J. Carpenter. January 1964. 37 p. incl. illus. (6121-7904-RU-000; BSD-TDR-64-16)
(Contract AF 04(694)-1) Unclassified report

A technique is developed for calculating rocket base heating and spacecraft heating environments due to particle radiation from a single nozzle rocket exhaust plume. The technique has proved successful when applied to a single nozzle exhausting into a rarefied atmosphere on the basis of comparison of predictions with experimental results.

The analysis treats radiation from a cloud of particles as that from an equivalent radiating surface. Thus, the problem is reduced to the
(over)

UNCLASSIFIED

UNCLASSIFIED

TRW Space Technology Laboratories Inc., One Space Park · Redondo Beach, California
THERMAL RADIATION FROM THE EXHAUST PLUME OF AN ALUMINIZED COMPOSITE PROPELLANT ROCKET, by S.J. Morizumi and H.J. Carpenter. January 1964. 37 p. incl. illus. (6121-7904-RU-000; BSD-TDR-64-16)
(Contract AF 04(694)-1) Unclassified report

A technique is developed for calculating rocket base heating and spacecraft heating environments due to particle radiation from a single nozzle rocket exhaust plume. The technique has proved successful when applied to a single nozzle exhausting into a rarefied atmosphere on the basis of comparison of predictions with experimental results.

The analysis treats radiation from a cloud of particles as that from an equivalent radiating surface. Thus, the problem is reduced to the
(over)

UNCLASSIFIED

determination of the proper values of the apparent surface emissivity and the effective temperature. The particle flow field information (particle concentrations, temperatures, and trajectories) necessary to determine these two quantities is provided by a two-phase flow field computer program developed by STL.

In defining the apparent emissivity of the particle plume, an analogy with neutron scattering for a cylindrical cloud is adopted which shows the apparent emissivity to be dependent on particle emissivity and cloud optical thickness. Since the plume is nonuniform in particle size, concentration, and temperature, certain averaging techniques are used to define mean values of optical thickness and temperature.

UNCLASSIFIED

UNCLASSIFIED

UNCLASSIFIED

determination of the proper values of the apparent surface emissivity and the effective temperature. The particle flow field information (particle concentrations, temperatures, and trajectories) necessary to determine these two quantities is provided by a two-phase flow field computer program developed by STL.

In defining the apparent emissivity of the particle plume, an analogy with neutron scattering for a cylindrical cloud is adopted which shows the apparent emissivity to be dependent on particle emissivity and cloud optical thickness. Since the plume is nonuniform in particle size, concentration, and temperature, certain averaging techniques are used to define mean values of optical thickness and temperature.

UNCLASSIFIED

determination of the proper values of the apparent surface emissivity and the effective temperature. The particle flow field information (particle concentrations, temperatures, and trajectories) necessary to determine these two quantities is provided by a two-phase flow field computer program developed by STL.

In defining the apparent emissivity of the particle plume, an analogy with neutron scattering for a cylindrical cloud is adopted which shows the apparent emissivity to be dependent on particle emissivity and cloud optical thickness. Since the plume is nonuniform in particle size, concentration and temperature, certain averaging techniques are used to define mean values of optical thickness and temperature.

UNCLASSIFIED

UNCLASSIFIED

UNCLASSIFIED

determination of the proper values of the apparent surface emissivity and the effective temperature. The particle flow field information (particle concentrations, temperatures, and trajectories) necessary to determine these two quantities is provided by a two-phase flow field computer program developed by STL.

In defining the apparent emissivity of the particle plume, an analogy with neutron scattering for a cylindrical cloud is adopted which shows the apparent emissivity to be dependent on particle emissivity and cloud optical thickness. Since the plume is nonuniform in particle size, concentration, and temperature, certain averaging techniques are used to define mean values of optical thickness and temperature.

UNCLASSIFIED